Discovery of Off-axis Jet Structure in TeV Blazar Mrk 501 by mm-VLBI

S. Koyama[1], M. Kino[2], M. Giroletti[3], A. Doi[4], K. Hada[3,5], E. Ros[1,6], K. Niinuma[7], H. Nagai[5], M. Orienti[3], G. Giovannini[3,8], T. Savolainen[1,9], T. P. Krichbaum[1], and M. A. Pérez-Torres[10,11]

Max-Planck-Institut für Radioastronomie

MAX-PLANCK-GESELLSCHAFT

1: Max Planck Institute for Radio Astronomy 2: Korea Astronomy and Space Science Institute 3: INAF Istituto di Radioastronomia 4: Institute of Space and Astronautical Science, Japan Aerospace Exploration Agency 5: National Astronomical Observatory of Japan 6: Universitat de València 7: Yamaguchi University 8: Università di Bologna 9: Aalto University Metsähovi Radio Observatory 10: IAA-CSIC 11: Centro de Estudios de la Física del Cosmos de Aragón

Summary: We present results from 43 GHz (VLBA, six epochs from 2012.2 to 2013.2) and 86 GHz (GMVA, one epoch in 2012.4) observations toward the basis of the jet in Mrk 501. The 43 GHz data analysis reveals a new jet feature located northeast of the radio core, with a flux density of several tens of mJy, perpendicularly to the jet axis. The 86 GHz image also shows an emission extended northeast of the core and a southeast jet feature. The spectrum of the radio core is flat, consistent with previous results, while that of northeast component is flat-to-steep, and that of southeast jet is flat-to-invert.

Background: Ultra-high resolution VLBI observations above 43 GHz have resolved the innermost jet perpendicular to the main jet, and revealed that the jet components have completely different position angles from the other inner jet components in several quasars (J1924-29: Lu et al. 2012; 3C 279: Lu et al. 2013). The physical origin of the off-axis jet structure must be related to the properties of the regions where the jet is formed, but is still far from being well understood.

The TeV blazar Mrk 501 is one of the best BL Lac Objects to resolve the innermost jet because of its proximity (z=0.034). This source shows irregularly different apparent jet directions in different scales (see Figures). These images show clear limb-bright structure, while they did not show off-axis jet structure at the innermost.

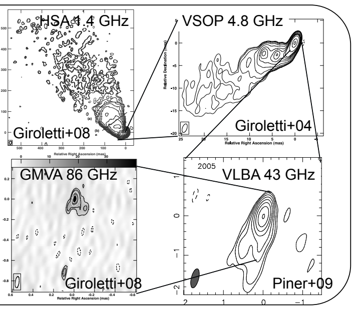

Observations and Results:

VLBA 43 GHz images

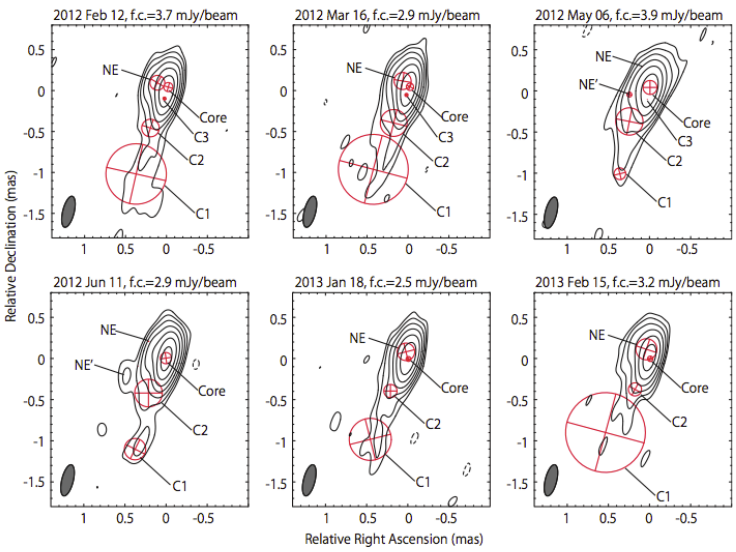

43 GHz uniform weighted VLBA CLEAN contour images with fitted circular Gaussian components. The common restoring beam is 0.39 mas x 0.14 mas in PA -14°, plotted in the bottom-left corner. Observing date and the first contour are plotted above each map. The first contours are set to three times the rms noise level of each map, increasing by a factor of 2.

Slice profiles of VLBA 43 GHz images along Core-NE

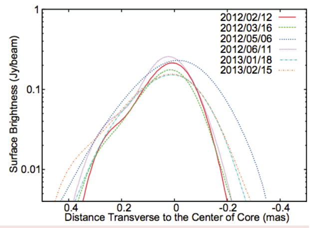

Slice profiles of the brightness along Gaussian center of the core and NE. The location of the Gaussian center is set to the reference position. All the profiles show clear asymmetry with an excess of emission to the East.

Gaussian models for slice profiles of VLBA 43 GHz images

Epoch	Model[a]	ID	Peak (mJy beam^{-1})	Position (mas)	FWHM (mas)	rms[b] (mJy)
BK172A	1	Core	208	...	0.20	158
	2	Core	207	...	0.17	25
	2	NE	39	0.16	0.21	
BK172B	1	Core	169	...	0.22	123
	2	Core	164	...	0.18	22
	2	NE	34	0.15	0.24	
BK172C	1	Core	227	...	0.31	93
	2	Core	215	...	0.27	29
	2	NE	36	0.18	0.30	
BK172D	1	Core	247	...	0.20	194
	2	Core	254	...	0.19	28
	2	NE	38	0.22	0.15	
BK172E	1	Core	150	...	0.28	70
	2	Core	137	...	0.23	16
	2	NE	40	0.16	0.24	
BK172F	1	Core	151	...	0.29	107
	2	Core	145	...	0.25	19
	2	NE	29	0.20	0.30	

(a) Fitting model type. Model 1 represents a single Gaussian model fitting. Model 2 represents a double Gaussian model fitting.
(b) Root sum squares of the residuals.

- The new component NE is located almost perpendicularly to the main jet axis (C1, C2, C3) for all the six epochs between 2012 Feb. and 2013 Feb.
- The location (angular separation, position angle, and flux) of NE changes randomly.
- Slice profiles show two humps, corresponding to the core and NE. The slice profiles are modeled by two Gaussian components (see details in Table above). For NE, the peak flux is 36 mJy/beam, the FWHM is 0.24 mas, at a core distance of 0.18 mas, in average.

GMVA 86 GHz

2012 May19

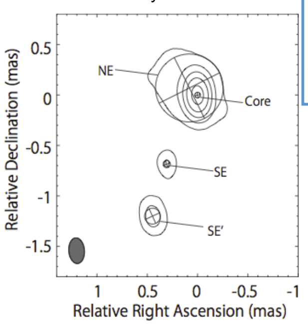

The GMVA image of Mrk 501 at 86 GHz with four circular Gaussian model components with the restoring beam of 0.26 mas × 0.16 mas in PA 4.41°. The peak brightness is 235 mJy/beam, and the contour levels are drawn at (-1, 1, 2, 4,...) x 10.7 mJy/beam. The 1σ noise level is 3.6 mJy/beam.

- The GMVA 86 GHz image shows an extended core emission (NE) at 0.11 mas northeast of the core.
- A southeast jet (SE) located at (r,θ)=(0.75 mas,156°) is also seen. The location could correspond to the one detected by the previous 86 GHz image obtained in 2008 May, located at (r,θ)=(0.73 mas, 172°) (Giroletti et al. 2008).
- A jet knot (SE') could correspond to C1 in the VLBA 43 GHz images.

Spectral index map and spectral profiles of 43 & 86 GHz

- The core region has a flat spectrum (α=0 ± 0.5). This is consistent with the core spectral indices of Mrk 501 derived so far (Giroletti et al. 2008, Hovatta et al. 2014).
- The NE region has a flat-to-steep spectrum (α=-0.8 ± 0.5). Though the spectral indices have large errors, NE could have steeper indices than the core does.
- The SE region has flat-to-inverted spectrum (α=0.6 ± 1.1). SE could have comparable or flatter spectral indices than the core does.
- We also took into account of the effect of core shift (~20 μas between 43 GHz and 86 GHz, extrapolated from the relation in Croke et al. 2008), however, the spectral tendency did not change.
- A flat-to-inverted jet spectrum could be due to shocks in the jets (Mimica et al. 2009), or superposition of multiple components along line of sight. The GMVA images of NRAO 150 at 86 GHz also show flat spectrum at jet components (Molina et al. 2014), but the non-simultaneous observations might cause large image misalignment due to structure change.

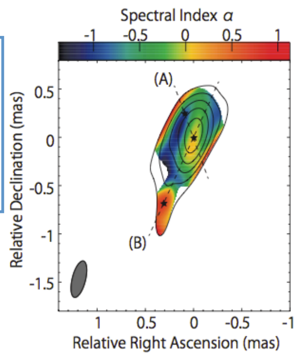

We define the flux density at observing frequency ν as $S_\nu \propto \nu^{+\alpha}$.

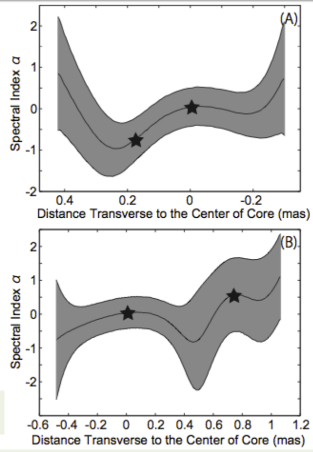

Left panel: Spectral index map between the third epoch VLBA 43 GHz map and the GMVA 86 GHz map. The contour map shows the VLBA 43 GHz map, with the contour levels drawn at (-1,1,2,4,…) x 9.0 mJy/beam, which is three times the rms noise of the off-source region of the 86 GHz image. Black dotted lines show the locations of the slices and black stars indicate the centroid positions of the fitted Gaussian components. Right panel: (A) Slice profile of spectral index along Gaussian center of the core and NE. The gray area indicates 1σ errors on the spectral index. The black starts show locations of the Gaussian components for the core and NE in the 43 GHz map. (B) Slice profile of spectral index map along Gaussian center of the core and SE. The black starts show locations of the Gaussian components for the core and SE in the 86 GHz map.

Future Prospects

Our observations cannot confirm the spectral index of the jet feature due to the limited sensitivity (512 Mbps) and (u,v)-coverage provided by the array used. To obtain more precise GMVA images, higher sensitivity (1 or 2 Gbps) and a better (u,v)-coverage, achievable by including new stations in the array, are recommended. Recently, the Korean VLBI Network joined the GMVA observations, therefore, it will increase the number of east-west baselines when there is no common sky between Europe and the USA. The east-west baselines ~9000 km are crucial for resolving the NE and core features with typically 50 μas resolution. Filling short baseline spacings will also enable us to perform more accurate calibration. Thus, the increased number of baselines is important for obtaining images and spectral index maps at higher fidelity.

References

Croke, S. M., O'Sullivan, S. P., & Gabuzda, D. C. 2010, MNRAS, 402, 259
Giroletti, M., Giovannini, G., Feretti, L., et al. 2004, ApJ, 600, 127
Giroletti, M., Giovannini, G., Cotton, W. D., et al. 2008, A&A, 488, 905
Hovatta, T., Aller, M. F., Aller, H. D., et al. 2014, AJ, 147, 143
Lu, R.-S., Fish, V. L., Akiyama, K., et al. 2013, ApJ, 772, 13
Lu, R.-S., Fish, V. L., Weintroub, J., et al. 2012, ApJ, 757, L14
Mimica, P., Aloy, M-A., Agudo, I., et al. 2009, ApJ, 696,1142
Molina, S. N., Agudo, I., Gómez, J. L., et al. 2014, A&A, 566, A26
Piner, B. G., Pant, N., Edwards, P. G., & Wiik, K. 2009, ApJ, 690, L31